

Antibacterial and Antifungal Polyketides from the Fungus *Aspergillus unguis* PSU-MF16

Praphatsorn Saetang, Vatcharin Rukachaisirikul,* Souwalak Phongpaichit, Sita Preedanon, Jariya Sakayaroj, Sarinya Hadsadee, and Siriporn Jungstittiwong



Cite This: *J. Nat. Prod.* 2021, 84, 1498–1506



Read Online

ACCESS |



Metrics & More

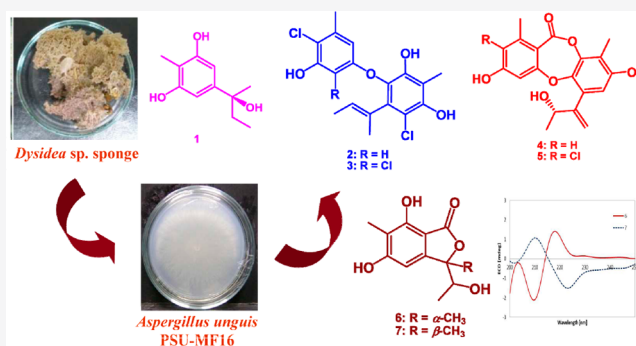


Article Recommendations



Supporting Information

ABSTRACT: Seven new polyketides including a phenol (**1**), two diphenyl ethers (**2** and **3**), two depsidones (**4** and **5**), and two phthalides (**6** and **7**) were isolated from the fungus *Aspergillus unguis* PSU-MF16 along with 27 known compounds. Their structures were determined by extensive spectroscopic analysis. The absolute configurations of **1** and **4**–**7** were established using comparative analyses of calculated and experimental ECD spectra. Among the new metabolites, **2** exhibited the best antimicrobial activity against *Staphylococcus aureus*, methicillin-resistant *S. aureus*, and *Microsporum gypseum* with equal MIC values of 16 $\mu\text{g/mL}$. In addition, known emeguisin A displayed potent antimicrobial activity against *S. aureus*, methicillin-resistant *S. aureus*, and *Cryptococcus neoformans* with equal MIC values of 0.5 $\mu\text{g/mL}$, compared with the standard drugs, vancomycin and amphotericin B. The structure–activity relationship study of the isolated compounds for antimicrobial activity is discussed.



B. The structure–activity relationship study of the isolated compounds for antimicrobial activity is discussed.

Previous investigations on secondary metabolites of the fungus *Aspergillus unguis* have provided unique types of polyketide metabolites including depsidones, depsides, diphenyl ethers, and phthalides.^{1–5} The depsidone derivatives showed a wide range of biological activities such as antiaromatase,² antibacterial,³ antimalarial,³ antifungal,⁵ and CFTR inhibitory⁵ activities, whereas depside and diphenyl ether derivatives displayed antifungal⁴ and antibacterial⁵ activities, respectively. As part of our research on antimicrobial metabolites from marine-derived fungi, we chemically investigated the fungus *Aspergillus unguis* PSU-MF16 isolated from a sponge in the genus *Dysidea* collected from Koh Bulon Mai Pai, Satun Province, Thailand. The culture broth EtOAc extract displayed antimicrobial activities against *Staphylococcus aureus*, methicillin-resistant *S. aureus*, and *Cryptococcus neoformans* with MIC values of 16, 16, and 4 $\mu\text{g/mL}$, respectively. In addition, the mycelial EtOAc extract was active against *S. aureus*, methicillin-resistant *S. aureus*, *C. neoformans*, and *Candida albicans* with the respective MIC values of 8, 8, 4, and 128 $\mu\text{g/mL}$, whereas the mycelial hexane extract displayed MIC values of 4, 4, 4, and 128 $\mu\text{g/mL}$ against the above human pathogens, respectively. In this study, we describe herein the isolation of one new phenol, aspergillusphenol C (**1**), and two new diphenyl ethers, aspergillusethers E (**2**) and F (**3**), together with 22 known compounds including seven depsidones, unguinol (**8**),^{5,6} 2-chlorounguinol (**9**),^{5,6} aspergillusidone C (**10**),^{1,5} normidulin (**11**),^{5,6} nidulin (**12**),^{5,6} aspergillusidone A (**13**),^{1,5} and aspergisidone (**14**),⁵ six depsides, asperlide (**15**),³ aspergisides

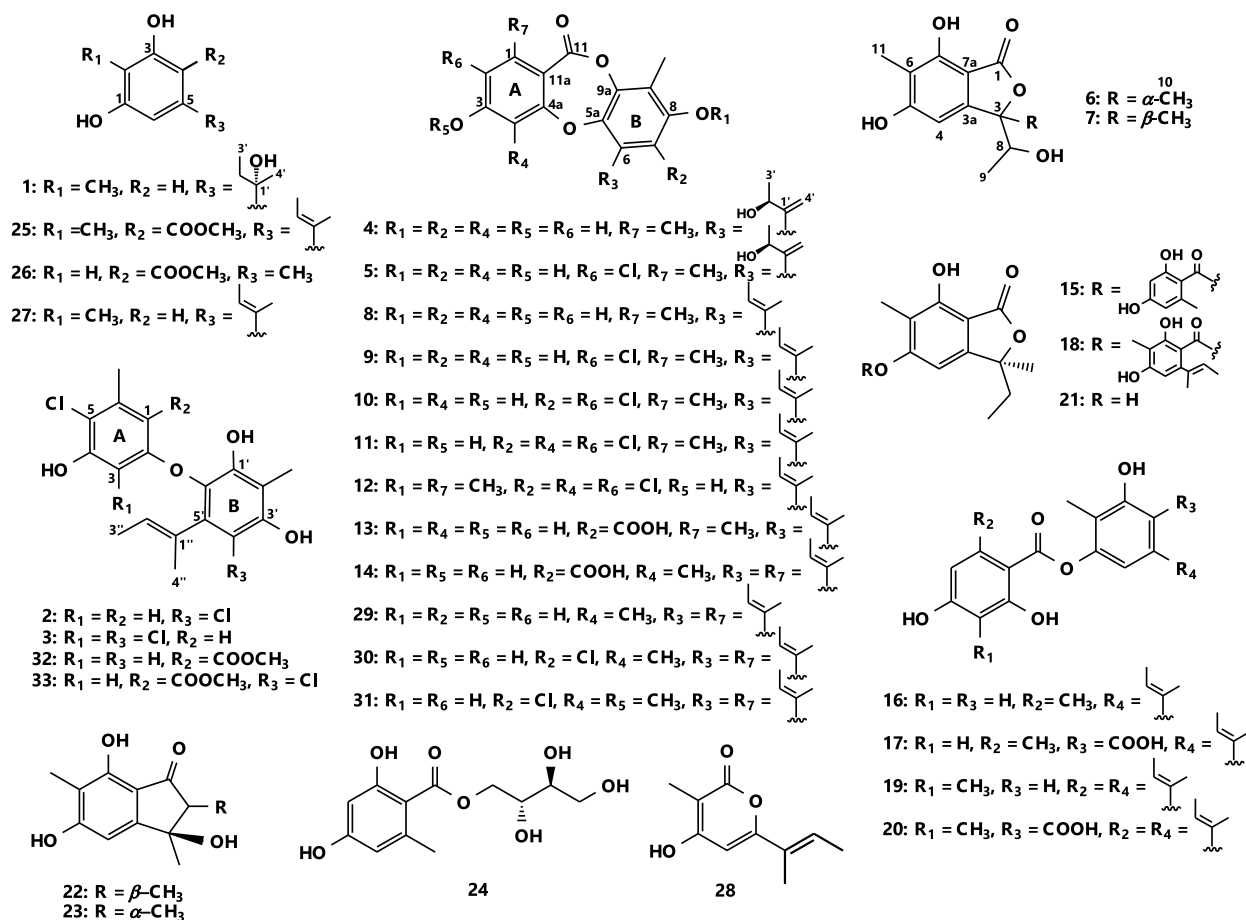
A–C (**16**–**18**),⁵ and agonodepsides A (**19**)⁷ and B (**20**),⁷ one phthalide, (3S)-3-ethyl-5,7-dihydroxy-3,6-dimethylphthalide (**21**),^{5,6} two indanones, asperunguisones A (**22**)⁴ and B (**23**),⁴ three orsellinic acid derivatives, (+)-montagnetol (**24**),^{4,8} pilobolusate (**25**),⁴ and methyl orsellinate (**26**),⁴ two phenols, aspergillusphenol A (**27**)^{2,4} and orcinol,⁴ and one pyranone, 4-hydroxy-3-methyl-6-(1-methyl-1-propenyl)-2H-pyran-2-one (**28**),¹ from the broth extract of *A. unguis* PSU-MF16. Moreover, two new depsidones, asperunguisidones A (**4**) and B (**5**), and two new phthalides, asperunguisides A (**6**) and B (**7**), as well as five additional known compounds including three depsidones, folipastatin (**29**),^{5,9} emeguisins A (**30**)^{5,10} and B (**31**),¹⁰ and two diphenyl ethers, aspergillusethers C (**32**)⁴ and D (**33**),⁴ were isolated from the mycelial EtOAc extract, whereas the mycelial hexane extract provided six previously isolated compounds (**8**–**10**, **29**, **30**, and **33**). The isolated compounds with sufficient quantity were evaluated for antibacterial (against *S. aureus* ATCC25923, methicillin-resistant *S. aureus*), antifungal (against *C. albicans* NCPF90028, *C. neoformans* ATCC90113, and *Microsporum*

Received: December 5, 2020

Published: April 16, 2021



Chart 1



gypseum, a clinical isolate) and cytotoxic (against African green-monkey fibroblasts and Vero cell lines) activities.

RESULTS AND DISCUSSION

The broth and mycelial extracts of *A. unguis* PSU-MF16 were purified using various chromatographic techniques, and the structures of the isolated compounds were elucidated on the basis of spectroscopic data including UV, IR, NMR, and MS. The relative configuration was assigned using NOEDIFF data, whereas the absolute configurations of **1** and **4–7** were determined by comparison of the experimental electronic circular dichroism (ECD) data with the calculated ones. For the known compounds, their structures were confirmed by comparison of the ^1H and ^{13}C NMR spectroscopic data as well as specific rotations with those previously reported.

Aspergillusphenol C (**1**) was obtained as a colorless gum with the molecular formula $\text{C}_{11}\text{H}_{16}\text{O}_3$ determined by the HRESIMS peak at m/z 197.1163 $[\text{M} + \text{H}]^+$. The IR spectrum showed hydroxy and double-bond absorption bands at 3385 and 1623 cm^{-1} , respectively. The UV spectrum exhibited absorption bands at 206 and 272 nm, indicating the presence of a benzene chromophore.² The ^1H and ^{13}C NMR spectroscopic data (Table 1) were similar to those of **27**² with the exception that proton signals for the 2-substituted-2-butenyl unit in **27** were replaced by signals for the 2-substituted-2-hydroxybutyl unit in **1**. The presence of signals for a hydroxy nonprotonated carbon (C-1', δ_{C} 74.3) and a methylene carbon (C-2', δ_{C} 37.7) in **1** instead of those for olefinic nonprotonated and olefinic methine carbons in **27**

supported the above conclusion. The 2-substituted-2-hydroxybutyl unit was constructed on the basis of the COSY correlations of the methylene protons, $\text{H}_2\text{-2}'$ (δ_{H} 1.69), and the methyl protons, $\text{H}_3\text{-3}'$ (δ_{H} 0.75) (Figure 1), and the HMBC correlations from the methyl protons, $\text{H}_3\text{-4}'$ (δ_{H} 1.39), to C-1' and C-2' (Figure 1) as well as the chemical shift of C-1' (Table 1). The HMBC correlations from $\text{H}_2\text{-2}'$ and $\text{H}_3\text{-4}'$ to C-5 (δ_{C} 148.4) confirmed the attachment of the 2-substituted-2-hydroxybutyl unit at this carbon. Accordingly, **1** was identified as a hydrated derivative of **27**. In order to determine the absolute configuration at C-1', the calculated ECD spectra of both enantiomers were performed using time-dependent density functional theory (TD-DFT) calculations. The experimental ECD spectrum of **1** displayed a similar shape of curves and Cotton effects to those of the calculated ECD spectrum of the *S* isomer (Figure 2). These results established the absolute configuration of **1** to be 1'*S*.

Aspergillusether E (**2**) was obtained as a colorless gum and had the molecular formula $\text{C}_{18}\text{H}_{18}\text{Cl}_2\text{O}_4$, which was deduced from the HRESIMS peak at m/z 391.0483 $[\text{M} + \text{Na}]^+$. It exhibited UV absorption bands of a benzene chromophore at 207 and 284 nm,² while the IR spectrum showed absorption bands at 3447 and 1604 cm^{-1} for hydroxy and double-bond functional groups, respectively.⁴ The ^1H NMR spectroscopic data (Table 1) were similar to those of **33**⁴ except for the replacement of signals for an aromatic proton and a methoxy group of ring A in **33** with those for two *meta*-coupled aromatic protons (δ_{H} 6.27, H-1, and 6.22, H-3) in **2**. The replacement of signals for one methyl ester group in **33** with a

Table 1. ^1H and ^{13}C NMR Data for 1–3

position	1^a		2^a		3^b	
	δ_{C} , type	δ_{H} (J in Hz)	δ_{C} , type	δ_{H} (J in Hz)	δ_{C} , type	δ_{H} (J in Hz)
1	156.7, C		110.2, CH	6.27, d (2.0)	109.0, CH	6.08, s
1-OH		7.86, brs				
2	109.0, C		158.7, C		152.8, C	
2-Me	8.5, CH_3	2.05, s				
3	156.7, C		102.5, CH	6.22, d (2.0)	107.9, C	
3-OH		7.86, brs				
4	104.8, CH	6.50, s	154.4, C		148.8, C	
4-OH				8.62, s		5.97, s
5	148.4, C		114.2, C		114.9, C	
6	104.8, CH	6.50, s	138.2, C		135.6, C	
6-Me			20.4, CH_3	2.26, s	20.2, CH_3	2.22, s
1'	74.3, C		148.6, C		146.8, C	
1'-OH				8.11, s		5.47, s
2'	37.7, CH_2	1.69, q (7.5)	112.8, C		111.2, C	
2'-Me			9.7, CH_3	2.19, s	9.3, CH_3	2.25, s
3'	8.8, CH_3	0.75, t (7.5)	149.6, C		148.1, C	
3'-OH				7.77, s		5.67, s
4'	30.6, CH_3	1.39, s	110.8, C		110.6, C	
5'			136.1, C		134.5, C	
6'			133.9, C		133.0, C	
1''			130.6, C		128.7, C	
2''			127.1, CH	5.22, qq (6.5, 1.5)	128.0, CH	5.27, q (7.0)
3''			13.7, CH_3	1.53, d (6.5)	13.7, CH_3	1.54, d (7.0)
4''			16.7, CH_3	1.68, s	16.4, CH_3	1.64, s

^aRecorded at 500 and 125 MHz for ^1H and ^{13}C in acetone- d_6 , respectively. ^bRecorded at 500 and 125 MHz for ^1H and ^{13}C in CDCl_3 , respectively.

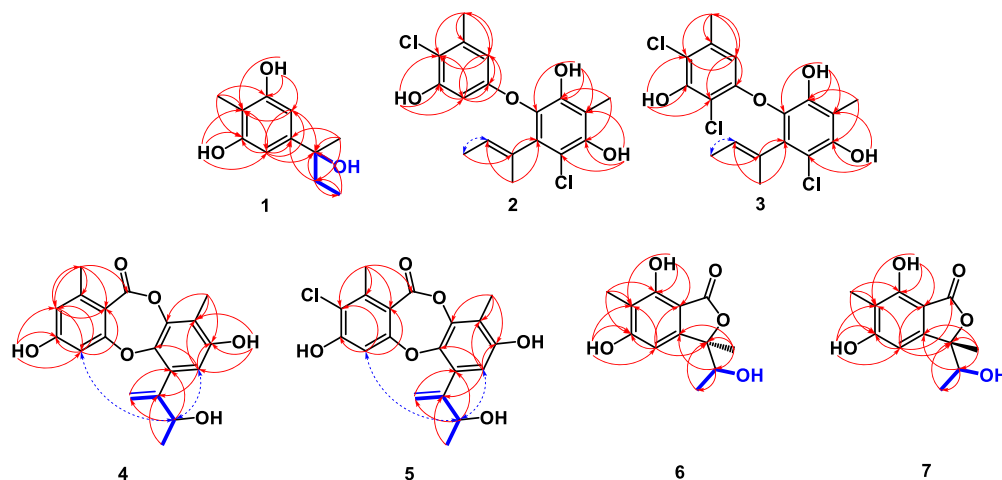


Figure 1. COSY (blue bars), key HMBC (red \curvearrowright), and NOEDIFF (blue \dashv) data of 1–7.

signal for an aromatic methine carbon in the ^{13}C NMR spectrum of **2** indicated that the methyl ester group at C-1 in **33** was replaced by an aromatic proton in **2**. This assignment was confirmed by the COSY correlation of H-1 (δ_{H} 6.27) with H-3 (δ_{H} 6.22) and the HMBC correlations from H-1 with C-2 (δ_{C} 158.7), C-3 (δ_{C} 102.5), C-5 (δ_{C} 114.2), and 6-Me (δ_{C} 20.4) (Figure 1). An *E*-configuration of the 2-substituted-2-butenyl unit was assigned according to signal enhancement of H₃-3'', but not H₃-4'', upon irradiation of H-2'' in the NOEDIFF experiment. Therefore, aspergillusether E had the structure **2**.

Aspergillusether F (**3**) was obtained as a colorless gum with the molecular formula $\text{C}_{18}\text{H}_{17}\text{Cl}_3\text{O}_4$ determined by the HRESIMS peak at m/z 403.0253 [$\text{M} + \text{H}$]⁺. The UV and

IR spectra of **3** were similar to those of **2**, indicating their identical chromophore and functional groups. The structural determination was accomplished by comparing its NMR spectroscopic data with those of **2**. The ^1H NMR spectrum of **3** (Table 1) differed from that of **2** in the replacement of signals for the two *meta*-coupled aromatic protons on ring A in **2** with an aromatic proton signal of a pentasubstituted benzene resonating at δ_{H} 6.08 (s, 1H) in **3**. This aromatic proton was assigned as H-1 based on its HMBC correlations with C-2 (δ_{C} 152.8), C-3 (δ_{C} 107.9), C-5 (δ_{C} 114.9), C-6 (δ_{C} 135.6), and 6-Me (δ_{C} 20.2) (Figure 1). A substituent at C-3 was assigned as a chlorine atom according to the chemical shift of C-3 and the molecular formula. Compound **3** displayed the NOEDIFF data (Figure 1) similar to those of **2**, indicating the identical

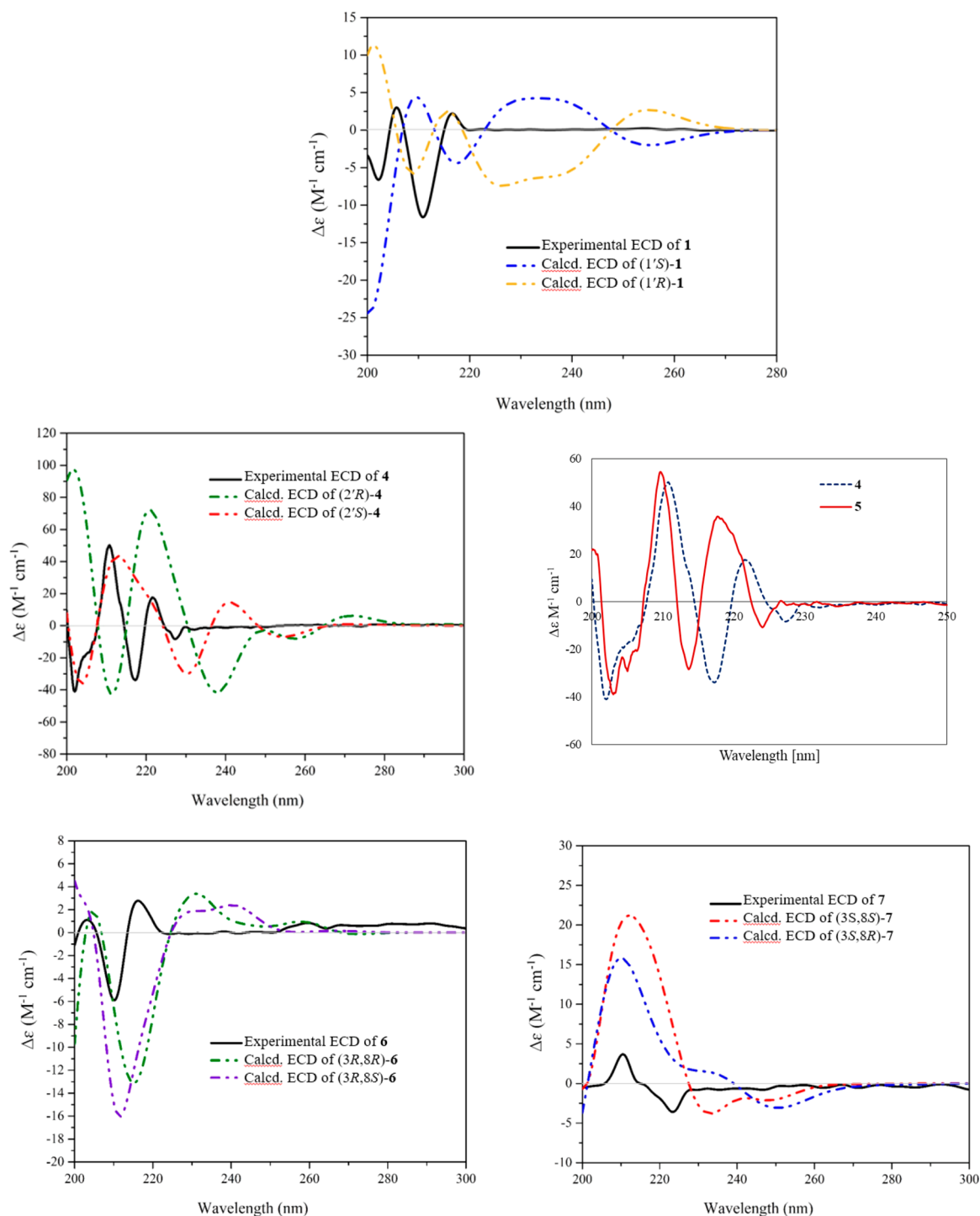


Figure 2. Experimental and calculated ECD spectra of **1**, **4**, **6**, and **7** and the experimental ECD spectrum of **5**.

configuration of the 2-substituted-2-butenyl unit. Therefore, **3** was identified as a 3-chloro derivative of **2**.

Asperunguissidone A (**4**) was isolated as a colorless gum and had the molecular formula $C_{19}H_{18}O_6$ on the basis of the HRESIMS peak at m/z 365.0998 $[M + Na]^+$. The UV absorption bands at 208 and 266 nm indicated the presence of a benzene chromophore. The IR spectrum displayed absorptions bands at 3357, 1707, and 1609 for hydroxy, ester carbonyl, and double-bond functional groups, respectively.¹ The 1H and ^{13}C NMR (Table 2), HMBC, and COSY (Figure 1) data revealed that **4** had a similar depsidone

structure to that of **8**.^{5,6} The obvious difference in the 1H NMR spectrum was the replacement of signals for the 2-substituted 2-butenyl unit in **8** with those for the 3-substituted-2-hydroxy-3-butenyl moiety in **4**. This unit was constructed on the basis of the COSY correlations of H-2' (δ_H 4.80) with H₃-3' (δ_H 1.18) (Figure 1) along with the HMBC correlations (Figure 1) from the geminal olefinic protons, H_{ab}-4' (δ_H 5.63 and 5.03), and H₃-3' to C-1' (δ_C 152.1) and C-2' (δ_C 70.0). The chemical shift of C-2' indicated the attachment of a hydroxy group at this carbon. This unit was attached at C-6 (δ_C 132.7) of the depsidone skeleton because H-2' and H_{ab}-4'

Table 2. ¹H and ¹³C NMR Data for 4 and 5 in Acetone-*d*₆

position	4 ^a		5 ^b	
	δ _C , type	δ _H (J in Hz)	δ _C , type	δ _H (J in Hz)
1	145.9, C		142.4, C	
1-Me	21.2, CH ₃	2.40, s	18.5, CH ₃	2.47, s
2	116.6, CH	6.63, d (2.1)	120.4, C	
3	162.6, C		158.1, C	
3-OH		9.51, s		
4	106.2, CH	6.56, d (2.1)	106.9, CH	6.83, s
4a	163.3, C		162.4, C	
5a	142.3, C		142.2, C	
6	132.6, C		132.7, C	
7	112.8, CH	6.58, s	112.9, CH	6.59, s
8	153.5, C		153.7, C	
8-OH		8.64, s		8.69, brs
9	117.0, C		117.0, C	
9-Me	9.6, CH ₃	2.17, s	9.5, CH ₃	2.17, s
9a	144.9, C		144.7, C	
11	164.7, C		163.1, C	
11a	113.8, C		115.6, C	
1'	152.1, C		151.9, C	
2'	70.0, CH	4.80, q (6.6)	70.0, CH	4.77, q (6.5)
3'	23.4, CH ₃	1.18, d (6.6)	23.3, CH ₃	1.18, d (6.5)
4'	114.0, CH ₂	a: 5.63, brt (1.8)	114.3, CH ₂	a: 5.63, brt (1.5)
		b: 5.03, dd (1.8, 0.9)		b: 5.03, s

^aRecorded at 300 and 75 MHz for ¹H and ¹³C, respectively.

^bRecorded at 500 and 125 MHz for ¹H and ¹³C, respectively.

gave HMBC correlations with this carbon. Signal enhancement of H-4 and H-7 after irradiation of H-2' in the NOEDIFF experiment (Figure 1) supported the assigned location. Based on the similar shape of curves and Cotton effects of the experimental ECD spectrum of 4 and the calculated ECD spectrum of the 2'-*S* isomer (Figure 2), asperunguissidone A had the depsidone structure 4 with an *S*-configuration at C-2'.

Asperunguissidone B (5) was isolated as a colorless gum and had the molecular formula C₁₉H₁₇ClO₆ on the basis of the HRESIMS peak at *m/z* 399.0607 [M + Na]⁺. The UV and IR spectra were similar to those of 4. In addition, their ¹H and ¹³C NMR spectroscopic data (Table 2) were similar except that signals for two *meta*-coupled aromatic protons on ring A of 4 were replaced by a signal for an aromatic proton of a pentasubstituted benzene resonating at δ_H 6.83 (s, 1H) in 5. This aromatic proton was assigned as H-4 on the basis of the HMBC correlations with C-2 (δ_C 120.4), C-3 (δ_C 158.1), C-4a (δ_C 162.4), and C-11a (δ_C 115.6) (Figure 1). The substituent at C-2 was assigned as a chlorine atom by comparison of the chemical shift of C-2 with that of previously reported chlorinated depsidones⁶ as well as the molecular formula. The absolute configuration at C-2' of 5 was assigned to be *S*, identical to that of 4, on the basis of their similar experimental ECD data (Figure 2). Consequently, 5 was assigned as a 2-chloro derivative of 4.

Asperunguislide A (6) was obtained as a colorless gum and had the molecular formula C₁₂H₁₄O₅ on the basis of the HRESIMS peak at *m/z* 261.0733 [M + Na]⁺. The UV spectrum exhibited absorption bands at 216, 262, and 296 nm, indicating the presence of a conjugated carbonyl chromophore.¹¹ The IR spectrum showed absorption bands for hydroxy, ester carbonyl, and double-bond functional groups at

3400, 1719, and 1618 cm⁻¹, respectively.¹⁴ The ¹H NMR spectroscopic data (Table 3) contained signals for two hydroxy

Table 3. ¹H and ¹³C NMR Data for 6 and 7 in Acetone-*d*₆

position	6 ^a		7 ^b	
	δ _C , type	δ _H (J in Hz)	δ _C , type	δ _H (J in Hz)
1	172.0, C		172.0, C	
3	90.6, C		90.8, C	
3a	152.0, C		152.6, C	
4	102.2, CH	6.63, s	101.9, CH	6.61, s
5	163.8, C		163.7, C	
5-OH		9.45, s		9.46, brs
6	111.7, C		111.7, C	
7	156.1, C		156.2, C	
7-OH		8.16, s		8.19, brs
7a	104.9, C		104.4, C	
8	72.0, CH	4.02, quint (6.0)	72.0, CH	3.90, quint (6.3)
8-OH		4.29, brd (6.0)		4.23, d (6.3)
9	17.9, CH ₃	1.04, d (6.0)	18.1, CH ₃	1.11, d (6.3)
10	23.2, CH ₃	1.59, s	21.6, CH ₃	1.57, s
11	7.9, CH ₃	2.08, s	7.8, CH ₃	2.08, s

^aRecorded at 500 and 125 MHz for ¹H and ¹³C, respectively.

^bRecorded at 300 and 75 MHz for ¹H and ¹³C, respectively.

protons (δ_H 9.45 and 8.16 each s, 1H), one aromatic proton of a pentasubstituted benzene (δ_H 6.63, s, 1H), one 1-substituted ethanol unit [δ_H 4.02 (quint, *J* = 6.0 Hz, 1H), 4.29 (brd, *J* = 6.0 Hz, 1H), and 1.04 (d, *J* = 6.0 Hz, 3H)], and two methyl groups (δ_H 2.08 and 1.59, each s, 3H). The ¹³C NMR spectrum (Table 3) displayed signals for one ester carbonyl (δ_C 172.0), six nonprotonated (δ_C 163.8, 156.1, 152.0, 111.7, 104.9, and 90.6), two methine (δ_C 102.2 and 72.0), and three methyl (δ_C 23.2, 17.9, and 7.9) carbons. These results together with the HMBC correlations (Figure 1) suggested that 6 had a similar phthalide skeleton to that of 21^{5,6} with the presence of the 1-substituted ethanol unit instead of an ethyl group in 21. A methylene carbon resonance in the ¹³C NMR spectrum in 21 was replaced by one oxymethine carbon resonance at δ_C 72.0 in 6, supporting the above conclusion. The COSY correlation of the hydroxymethine proton (H-8, δ_H 4.02) with H₃-9 (δ_H 1.04) and the HMBC cross-peaks of H-8 with C-3a (δ_C 152.0) (Figure 1) confirmed the presence of the 1-substituted ethanol unit and further established the attachment of the this unit at C-3. The determination of the absolute configuration at C-8 by the modified Mosher's method was not performed because of insufficient material. In the ECD spectrum, 6 displayed a negative Cotton effect (Δε -2.1) at 210 nm (Figure 2) which had an opposite sign to that of 15 (211 nm, Δε +28.21),³ 18 (213 nm, Δε +5.51),⁵ and 21 (213 nm, Δε +5.84).⁵ These results suggested an *R*-configuration at C-3. Accordingly, the absolute configuration of 6 would be either 3*R*,8*R* or 3*R*,8*S*. The ECD calculations afforded the calculated spectra that did not allow for definitive assignment of the configuration at C-8 (Figure 2). Based on these data, the absolute configuration at C-8 remained unidentified.

Asperunguislide B (7) was obtained as a colorless solid. It had an identical molecular formula to that of 6 based on the HRMS peak at *m/z* 261.0737 [M + Na]⁺. The UV and IR absorption bands were similar to those of 6. The ¹H, and ¹³C NMR (Table 3), COSY, and HMBC (Figure 1) data of 7 indicated that 7 had an identical planar structure to 6. The absolute configuration at C-3 was determined to be *S* on the

Table 4. Antibacterial, Antifungal, and Cytotoxic Activities of 2, 4, 6–21, 24–27, and 29–33

compound	antibacterial activity (MIC, $\mu\text{g/mL}$)		antifungal activity (MIC, $\mu\text{g/mL}$)			cytotoxicity (IC_{50} , μM)
	<i>S. aureus</i>	methicillin-resistant <i>S. aureus</i>	<i>C. albicans</i>	<i>C. neoformans</i>	<i>M. gypseum</i>	Vero
2	16	16	32	32	16	130
4	64	64	– ⁱ	–	–	ND ^j
6	–	–	–	–	200	ND
7	–	–	–	–	–	ND
8 ^a	128	–	–	200	–	–
9 ^a	8	8	8	32	8	86
10 ^a	2	1	200	128	2	8.9
11 ^a	2	2	–	8	–	110
12 ^a	4	8	–	16	–	57
13 ^a	–	–	–	200	–	–
14 ^a	32	64	–	64	200	–
15	200	200	–	32	200	–
16 ^a	8	8	200	64	128	84
17 ^a	128	128	–	32	–	110
18 ^a	200	200	–	200	–	45
19	2	2	–	32	32	38
20	8	16	128	32	8	–
21 ^a	2	4	128	32	8	40
24 ^b	–	–	–	200	–	–
25 ^b	64	64	200	64	128	77
26 ^b	–	–	–	200	–	–
27 ^b	16	8	–	128	128	130
29 ^a	2	1	–	1	–	17
30 ^a	0.5	0.5	–	0.5	–	16
31	–	–	–	–	–	ND
32 ^b	64	64	128	64	128	36
33 ^b	64	128	16	8	–	110
control	0.5 ^c	1.0 ^d	0.5 ^e	2.0 ^f	2.0 ^g	4.0 ^h

^aValues from ref 5. ^bValues from ref 4. ^c*S. aureus*: vancomycin; MIC 0.25 $\mu\text{g/mL}$ for 8–14, 16–19, 21, 24–27, 29, 30, 32, and 33. ^dMethicillin *S. aureus*: vancomycin; MIC 0.5 $\mu\text{g/mL}$ for 4, 8–15, 16–18, 20, 21, 24–27, 29, 30, 32, and 33; MIC 0.25 $\mu\text{g/mL}$ for 19. ^e*C. albicans*: amphotericin B; MIC 0.25 $\mu\text{g/mL}$ for 4, 8–14, 16–18, 21, 24–27, 29, 30, 32, and 33. ^f*C. neoformans*: amphotericin B; MIC 0.5 $\mu\text{g/mL}$ for 4, 15, and 20; MIC 0.25 $\mu\text{g/mL}$ for 8–14, 16–19, 21, 24–27, 29, 30, 32, and 33. ^g*M. gypseum*: clotrimazole; MIC 1.0 $\mu\text{g/mL}$ for 8–14, 16–18, 21, 24–27, 29, 30, 32, and 33; MIC 0.5 $\mu\text{g/mL}$ for 4, 15, and 20; MIC 0.25 $\mu\text{g/mL}$ for 19. ^hVero: ellipticine; IC_{50} 4.6 μM for 8–14, 16–18, 21, 24–27, 29, 30, 32, and 33; IC_{50} 5.5 μM for 15 and 20. ⁱ– = inactive at the concentration of 50 $\mu\text{g/mL}$. ^jND = not determined.

basis of a positive Cotton effect at 210 nm in the ECD spectrum (Figure 2), the same sign as that of 15, 18, and 21. Consequently, the absolute configuration of 7 would be either 3S,8S or 3S,8R. As 6 and 7 were separable by normal-phase PTLC, they were diastereomers, not a pair of enantiomers. Attempts to prepare the Mosher's esters resulted in the decomposition of material. The ECD calculations provided inadequate data for the assignment of the absolute configuration at C-8 (Figure 2). Therefore, 7 is the C-3 epimer of 6, but the C-8 configuration remains unassigned.

The antimicrobial activities of compounds 8–14, 16–18, 21, 24–27, 29, 30, 32, and 33 against *S. aureus* ATCC25923, methicillin-resistant *S. aureus*, *C. albicans* NCPF90028, *C. neoformans* ATCC90113, and *M. gypseum* were previously reported by our research group (Table 4).^{4,5} In addition, these compounds were noncytotoxic to Vero cells (Table 4).^{4,5} Accordingly, compounds 2, 4, 6, 7, 15, 19, 20, and 31 with sufficient amount were evaluated for antimicrobial activity against the same pathogens (Table 4). Among the diphenyl ether derivatives (2, 32, and 33), 2, without the methyl ester group at C-1, showed stronger activity against *S. aureus*, methicillin-resistant *S. aureus*, and *M. gypseum* than the corresponding methyl ester 33⁴ with equal MIC values of 16 $\mu\text{g/mL}$. In contrast, 2 was 2- and 4-fold less active than 33

against *C. albicans* and *C. neoformans*, respectively.⁴ It is worth noting that the nonchlorinated diphenyl ether 32 was less active against *C. albicans* and *C. neoformans*, but more active against methicillin-resistant *S. aureus* and *M. gypseum* than 33.⁴ These results indicated that the methyl ester group at C-1 and the chlorine atom at C-4' played an important role for antimicrobial activity.

For the phthalides (6, 7, 15, 18, and 21), compound 6, the 8-hydroxy derivative of 21, and 7, the C-3 epimer of 6, were inactive in antimicrobial assays. Compound 21 displayed interesting antibacterial (MIC values 2–4 $\mu\text{g/mL}$) and weak to moderate antifungal (MIC values 8–128 $\mu\text{g/mL}$) activities.⁵ In addition, 15 and 18,⁵ the benzoate derivatives of 21, displayed much weaker antimicrobial activity than 21. Based on these data, a hydroxy group at C-5, but not the one at C-8, enhanced the activity.

Among the tested depside derivatives (16, 17, 19, and 20), 19 displayed the strongest activity against *S. aureus* and methicillin-resistant *S. aureus* with equal MIC values of 2 $\mu\text{g/mL}$, whereas 20, the carboxy derivative of 19, was the most active against *M. gypseum*, with an MIC value of 8 $\mu\text{g/mL}$. In addition, 16 displayed much better activity against all tested pathogens, except for *C. neoformans*, than the corresponding carboxy derivative 17.⁵ However, 16 was less active against all

tested pathogens, except for *C. albicans*, than 19. These results indicated that the antimicrobial activity of these depsides was controlled by the presence of a carboxyl moiety, the position of the methyl group on ring A, and the number of 2-substituted 2-butenyl units.

The tested depsidones can be divided into two types. The first type is 1-methyl-6-(2-methylbut-2-enyl)depsidone derivatives (4 and 8–13), whereas the second type is 4-methyl-1,6-di(2-methylbut-2-enyl)depsidone derivatives (14 and 29–31). All metabolites of the first depsidone type, except for nonchlorinated 4, 8, and 13, displayed significant antibacterial activity against both bacterial strains with the MIC values in the range of 1–8 $\mu\text{g}/\text{mL}$.⁵ These results revealed that the chlorine substituents at C-2, C-4, and C-7 dramatically enhanced antibacterial activity. Interestingly, an additional chlorine atom at C-4 in 11 and 12 remarkably increased the antifungal activity against *C. neoformans* when compared with 10. Moreover, 4 differing from 8 in the presence of the 3-substituted-2-hydroxy-3-butenyl moiety instead of the 2-methylbut-2-enyl unit, was active against methicillin-resistant *S. aureus* and displayed 2-fold more activity than 8 against *S. aureus*. In contrast, the replacement of H-7 in 8 with a carboxyl group in 13 resulted in no antibacterial activity. For the second depsidone type, the nonchlorinated 29 was much more potent than 8 from the first type against *S. aureus*, methicillin-resistant *S. aureus*, and *C. neoformans* with the respective MIC values of 2, 1, and 1 $\mu\text{g}/\text{mL}$.⁵ But 14, the carboxyl derivative of 29, was 16-, 64-, and 64-fold less active than 29 against the same pathogens, respectively. Again, 30, the 7-chloro derivative of 29, exhibited much better antibacterial and antifungal activities against the above pathogens than 29 with equal MIC values of 0.5 $\mu\text{g}/\text{mL}$.⁵ Additionally, the disappearance of antimicrobial activity of 31, the corresponding 3-methoxy derivatives of 30, suggested the importance of a 3-hydroxy group in these activities.

Finally, the antimicrobial 2, 15, 19, and 20, which were obtained in sufficient amount, were tested for cytotoxic activity against the Vero cell line. Compounds 15 and 20 were inactive at the concentration of 50 $\mu\text{g}/\text{mL}$, whereas compounds 2 and 19 were considered to be noncytotoxic to Vero cells with IC_{50} values of >10 μM .

In summary, the fungus *A. unguis* PSU-MF16 produced seven new (1–7) and 27 known polyketides. Depsidone derivatives are obtained as major metabolites. There are only two reports on the isolation of chlorinated diphenyl ether derivatives from *A. unguis*,^{1,4} while the depsidone derivatives bearing a 3-substituted-2-hydroxy-3-butenyl moiety at C-6 have never been reported. Accordingly, the diphenyl ether (2 and 3) and depsidone (4 and 5) derivatives are rare fungal metabolites. Among the tested polyketides, 10, 11, 19, 29, and 30 displayed interesting antibacterial activity against *S. aureus* and methicillin-resistant *S. aureus* with MIC values in the range 0.5–2 $\mu\text{g}/\text{mL}$. Compounds 29 and 30 were also strongly active against *C. neoformans* with respective MIC values of 1 and 0.5 $\mu\text{g}/\text{mL}$. Interestingly, among the tested compounds, 10 showed the strongest antifungal activity against *M. gypseum* with the MIC value of 2 $\mu\text{g}/\text{mL}$. In addition, antimicrobial activities of known compounds 15, 19, and 20 are reported for the first time.

EXPERIMENTAL SECTION

General Experimental Procedures. The specific rotations were performed with a JASCO P-2000 polarimeter. The ultraviolet

absorption spectra were measured in MeOH on a Shimadzu UV-2600 UV–vis spectrophotometer. ECD spectra were recorded on a JASCO J-815 polarimeter. The infrared spectra were recorded neat using a PerkinElmer 783 FTS165 FT-IR spectrometer. The ¹H and ¹³C NMR spectra were recorded on a 300 or a 500 MHz Bruker FTNMR Ultra Shield spectrometer using tetramethylsilane as an internal standard. ESI-TOF mass spectra were measured on a TOF/Q-TOF mass spectrometer. Thin-layer chromatography (TLC) and preparative TLC (PTLC) were performed on silica gel 60 GF₂₅₄ (Merck). Column chromatography (CC) was carried out on Sephadex LH-20, silica gel (Merck) type 60 (230–400 mesh ASTM) or type 100 (70–230 mesh ASTM), or reversed-phase C₁₈ silica gel.

Fungal Material. The fungus PSU-MF16 was isolated from a sponge in the genus *Dysidea* that was collected from Koh Bulon Mai Pai, Satun Province, Thailand. This fungus was deposited as BCC83151 at BIOTEC Culture Collection (BCC), National Center for Genetic Engineering and Biotechnology (BIOTEC), Thailand. The fungus PSU-MF16 was identified based on its morphological and molecular characteristics. Colonies on potato dextrose agar at 25 °C grew fast, reaching 4.2 cm in 7 days. Colony color is green. It produced a globose conidial head bearing phialides, which are the characteristics of the genus *Aspergillus*.¹² The molecular analysis of the rDNA sequence of the internal transcribed spacers (GenBank accession no. KY397987) through the BLAST search from GenBank revealed that PSU-MF16 matched with several nucleotides of *Aspergillus unguis* strains comprising *A. unguis*, KU866670, KU866641, KU866620, KU866616, and KU866612 (100% nucleotide similarity). Therefore, this fungus was then identified to be *A. unguis*.

Fermentation, Extraction, and Purification. The fermentation and extraction of the fungus *A. unguis* PSU-MF16 were carried out using the same procedure as described previously.¹³ The broth EtOAc extract (1.7 g, brown gum) was subjected to CC over Sephadex LH-20 using MeOH as a mobile phase to obtain nine fractions (A1–A9). Fraction A5 (90.3 mg) was subjected to CC over silica gel using a gradient of MeOH/CH₂Cl₂ (1:99–100:0) as a mobile phase to yield six subfractions (A5A–A5F). Purification of subfraction A5B (38.2 mg) using PTLC with a mixture of MeOH/CH₂Cl₂ (1:99) (two runs) afforded 18 (7.2 mg) and 21 (18.5 mg). Purification of subfraction A5D (5.0 mg) was performed by PTLC using a mixture of acetone/hexane (3:7) (five runs) to afford 28 (2.0 mg). Subfraction A5E (8.7 mg) was purified by CC over reversed-phase C₁₈ silica gel using a gradient of MeOH/H₂O (3:2–5:0) to afford five subfractions (A5E1–A5E5). Subfraction A5E2 contained 1 (1.2 mg). Compound 22 (1.4 mg) was obtained from subfraction A5E4 (2.6 mg) after purification by PTLC using a mixture of acetone/hexane (1:4) (eight runs). Purification of fraction A6 (192.4 mg) using the same procedure as fraction A5 gave eight subfractions (A6A–A6H). Subfraction A6G (15.3 mg) was purified by CC over reversed-phase C₁₈ silica gel with a gradient of MeOH/H₂O (3:2–5:0) to afford 23 (2.3 mg). Using the same procedure as fraction A5, fraction A8 (464.1 mg) gave 10 subfractions (A8A–A8J). Purification of subfraction A8A (22.8 mg) was performed by flash column chromatography (FCC) over silica gel with a mixture of acetone/hexane (1:4) to afford eight subfractions (A8A1–A8A8). Subfraction A8A1 (13.1 mg) yielded 25 (7.4 mg) upon purification on PTLC using a mixture of acetone/hexane (1:4) (seven runs). Subfractions A8A2 and A8A8 contained 3 (1.4 mg) and 12 (3.0 mg), respectively. Compound 2 (3.5 mg) was obtained from subfraction A8A4 (4.6 mg) using PTLC with a mixture of acetone/hexane (1:4) (five runs). Using the same purification procedure as subfraction A8A, subfraction A8C (47.1 mg) yielded four subfractions (A8C1–A8C4). Subfraction A8C2 (29.6 mg) was purified by FCC over silica gel using a mixture of acetone/hexane (1:4) followed by PTLC with a mixture of EtOAc/hexane (1:4) (five runs) to give 19 (3.5 mg). Purification of subfraction A8E (90.0 mg) by dissolving with CHCl₃ afforded a soluble subfraction (12.6 mg), which was further purification by PTLC with a mixture of acetone/hexane (1:4) (eight runs) to give 15 (6.1 mg). Subfraction A8F (14.9 mg) was dissolved with CHCl₃ to give a soluble subfraction, which

contained **8** (8.5 mg). Subfraction A8H (27.5 mg) was purified by CC over reversed-phase C_{18} silica gel with a gradient of MeOH/H₂O (3:2) followed by PTLC with a mixture of EtOAc/hexane (1:4) (four runs) to give orcinol (5.8 mg). Subfraction A8I (91.0 mg) was fractionated using the same procedure as subfraction A6G to give eight subfractions (A8I1–A8I8). Subfraction A8I1 (11.2 mg) gave **24** (6.2 mg) upon purification on PTLC using a mixture of CH₂Cl₂/EtOAc/MeOH (8:1:1) (two runs). Subfraction A8I3 contained **14** (6.3 mg), while subfraction A8I4 (6.0 mg) was subjected to PTLC with a mixture of MeOH/CH₂Cl₂ (1:49) (three runs) to afford **27** (1.8 mg). Using the same procedure as subfraction A8I, subfraction A8I7 (18.3 mg) provided **20** (4.8 mg). Fraction A9 (561.7 mg) was purified using the same procedure as fraction A5 to give nine subfractions (A9A–A9I). Compound **10** (18.4 mg) was obtained from subfraction A9A (79.0 mg) upon purification on FCC over silica gel with a mixture of EtOAc/CH₂Cl₂ (1:1). Subfraction A9B (38.4 mg) was fractionated by FCC over silica gel with a mixture of acetone/hexane (1:4) to provide **11** (5.2 mg). Compounds **9** (19.9 mg) and **26** (5.8 mg) were obtained from subfraction A9C (176.9 mg) upon purification by CC over silica gel using the same eluting system as subfraction A9B. Purification of subfraction A9H (157.5 mg) by the same procedure as subfraction A6G yielded eight subfractions (A9H1–A9H8). Subfraction A9H2 (19.8 mg) afforded **13** (7.6 mg) upon purification by CC over reversed-phase C_{18} silica gel with a mixture of MeOH/H₂O (1:1). Compound **17** (2.6 mg) was obtained from subfraction A9H5 (61.9 mg) upon purification by CC over reversed-phase C_{18} silica gel with a mixture of MeOH/H₂O (3:2) followed by CC over reversed-phase C_{18} silica gel with a mixture of MeOH/H₂O (2:3). Subfraction A9H8 contained **16** (2.8 mg).

The mycelial EtOAc extract (7.4 g, yellow solid) was purified by CC over Sephadex LH-20 using pure MeOH as a mobile phase to give four fractions (B1–B4). Fraction B2 (162.9 mg) was purified by the same procedure as fraction A5 to give eight subfractions (B2A–B2H). Subfraction B2H (31.2 mg) was purified by CC over reversed-phase C_{18} silica gel using a gradient of MeOH/H₂O (6:4–10:0) followed by PTLC with a mixture of hexane/EtOAc/MeOH (20:9:1) as a mobile phase (nine runs) to give **6** (3.5 mg) and **7** (3.8 mg). Purification of fraction B3 (5.5 g) using the same procedure as fraction B2 yielded 12 subfractions (B3A–B3L). Compound **31** (3.2 mg) was obtained from subfraction B3A (20.3 mg) upon purification on CC over silica gel with a mixture of EtOAc/hexane (1:9) followed by PTLC using a mixture of EtOAc/hexane (1:19) (four runs). Subfraction B3D (369.8 mg) was subjected to CC over reversed-phase C_{18} silica gel using a gradient of MeOH/H₂O (7:3–10:0) followed by FCC over silica gel using a mixture of EtOAc/hexane (1:9) to yield **33** (30.9 mg). Subfraction B3E (844.1 mg) was purified by dissolving with hexane to yield a soluble subfraction (55.2 g), which was further purified using CC over reversed-phase C_{18} silica gel with a gradient of MeOH/H₂O (7:3–10:0) to afford five subfractions (B3E1A–B3E1E). Subfraction B3E1E (108.1 mg) was fractionated by FCC over silica gel with a mixture of hexane/CH₂Cl₂ (3:7) to give **30** (25.9 mg). Subfraction B3F (835.7 mg) was subjected to CC over silica gel using the same procedure as fraction B2 to yield five subfractions (B3F1–B3F5). Compound **29** (33.7 mg) was obtained from subfraction B3F4 (606.4 mg) after purification by CC over silica gel with a mixture of MeOH/CH₂Cl₂ (1:99–100:0), subsequent FCC over silica gel with a mixture of acetone/hexane (1:4), followed by CC over reversed-phase C_{18} silica gel with a gradient of MeOH/H₂O (7:3–10:0). Subfraction B3H (123.5 mg) was further purified by CC over reversed-phase C_{18} silica gel using a mixture of MeOH/H₂O (3:2) followed by PTLC with a mixture of EtOAc/hexane (1:3) to give **32** (6.5 mg). Subfraction B3J (55.2 mg) was fractionated by CC over reversed-phase C_{18} silica gel with a gradient of MeOH/H₂O (1:1–2:0) to provide six subfractions (B3J1–B3J6). Compounds **4** (2.7 mg) and **5** (1.7 mg) were obtained from subfractions B3J3 (10.1 mg) and B3J5 (5.0 mg), respectively, after purification by PTLC with a mixture of CH₂Cl₂/hexane/MeOH (25:24:1) (five runs).

The mycelial hexane extract (1.5 g, pale yellow gum) was purified by various chromatographic techniques to give **8–10**, **29**, **30**, and **33** (see Supporting Information).

Aspergillusphenol C (1): colorless gum; $[\alpha]_D^{26}$ -3.7 (c 1.09, MeOH); UV (MeOH) λ_{max} nm ($\log \epsilon$) 206 (4.19), 272 (3.13); ECD (MeOH, 0.39 mM) λ_{max} ($\Delta\epsilon$) 202 (-6.7), 206 ($+2.8$), 211 (-11.7), 217 ($+2.0$) nm; IR (neat) ν_{max} cm⁻¹: 3385, 1623; ¹H and ¹³C NMR data, Table 1; HRESIMS m/z $[M + H]^+$ 197.1163 (calcd for C₁₁H₁₇O₃, 197.1172).

Aspergillusether E (2): colorless gum; UV (MeOH) λ_{max} nm ($\log \epsilon$) 207 (5.00), 284 (4.03); IR (neat) ν_{max} cm⁻¹ 3447, 1604; ¹H and ¹³C NMR data, Table 1; HRESIMS m/z $[M + Na]^+$ 391.0483 (calcd for C₁₈H₁₈Cl₂O₄Na, 391.0474).

Aspergillusether F (3): colorless gum; UV (MeOH) λ_{max} nm ($\log \epsilon$) 208 (4.59), 284 (3.58); IR (neat) ν_{max} cm⁻¹ 3432, 1607; ¹H and ¹³C NMR data, Table 1; HRESIMS m/z $[M + H]^+$ 403.0253 (calcd for C₁₈H₁₈Cl₃O₄, 403.0265).

Asperunguisidone A (4): colorless gum; $[\alpha]_D^{26}$ $+67.3$ (c 0.1, MeOH); UV (MeOH) λ_{max} nm ($\log \epsilon$) 208 (4.28), 266 (3.74); ECD (MeOH, 0.16 mM) λ_{max} ($\Delta\epsilon$) 202 (-40.9), 210 ($+49.4$), 216 (-33.9), 221 ($+16.2$), 227 (-8.2) nm; IR (neat) ν_{max} cm⁻¹ 3357, 1707, 1609; ¹H and ¹³C NMR data, Table 2; HRESIMS m/z $[M + Na]^+$ 365.0998 (calcd for C₁₉H₁₈O₆Na, 365.0996).

Asperunguisidone B (5): colorless gum; $[\alpha]_D^{26}$ $+39.3$ (c 0.1, MeOH); UV (MeOH) λ_{max} nm ($\log \epsilon$) 208 (4.58), 266 (3.89); ECD (MeOH, 0.16 mM) λ_{max} ($\Delta\epsilon$) 203 (-39.0), 210 ($+54.4$), 214 (-28.4), 218 ($+34.8$), 224 (-10.6) nm; IR (neat) ν_{max} cm⁻¹ 3400, 1708, 1597; ¹H and ¹³C NMR data, Table 2; HRESIMS m/z $[M + Na]^+$ 399.0607 (calcd for C₁₉H₁₇ClO₆Na, 399.0606).

Asperunguislide A (6): colorless gum; $[\alpha]_D^{26}$ $+252.6$ (c 0.05, MeOH); UV (MeOH) λ_{max} nm ($\log \epsilon$) 216 (4.40), 262 (4.25), 296 (3.80); ECD (MeOH, 2.0 mM) λ_{max} ($\Delta\epsilon$) 210 (-2.1), 218 ($+1.4$) nm; IR (neat) ν_{max} cm⁻¹ 3400, 1719, 1618; ¹H and ¹³C NMR data, Table 3; HRESIMS m/z $[M + Na]^+$ 261.0733 (calcd for C₁₂H₁₄O₅Na, 261.0733).

Asperunguislide B (7): colorless solid; $[\alpha]_D^{26}$ $+57.5$ (c 0.29, MeOH); UV (MeOH) λ_{max} nm ($\log \epsilon$) 216 (4.23), 262 (4.06), 296 (3.64); ECD (MeOH, 2.0 mM) λ_{max} ($\Delta\epsilon$) 210 ($+1.1$), 223 (-1.5) nm; IR (neat) ν_{max} cm⁻¹ 3284, 1719, 1618; ¹H and ¹³C NMR data, see Table 3; HRESIMS m/z $[M + Na]^+$ 261.0737 (calcd for C₁₂H₁₄O₅Na, 261.0733).

TD-DFT Calculations of the ECD Spectra. The optimized structure was performed by the DFT method at the B3LYP/6-311G(d,p) level of theory. The minima of structures using vibrational analysis at the B3LYP/6-311G(d,p) level of theory resulted in no imaginary frequencies. ECD spectra was carried out using the TD-DFT method at the B3LYP/6-311++G(d,p) level. The rotary strengths of 60 excited states were determined. All calculations were performed using the Gaussian09 program package. A Gaussian band shape with a bandwidth of 0.20 eV was used to simulate the ECD spectra. The ECD curves were generated by the software SpecDis 1.64 (University of Wurzburg, Wurzburg, Germany).¹⁴

Antimicrobial Assay. Antimicrobial activity was determined as described by the Clinical and Laboratory Standards Institute.¹⁵ The positive controls were vancomycin for both *S. aureus* and methicillin-resistant *S. aureus*, amphotericin B for *C. albicans* and *C. neoformans*, and clotrimazole for *M. gypseum*.

Cytotoxicity Assay. Cytotoxic activity against African green monkey kidney fibroblast (Vero) cells was assessed employing the colorimetric method.¹⁶ Ellipticine was used as a positive control.

■ ASSOCIATED CONTENT

Supporting Information

The Supporting Information is available free of charge at <https://pubs.acs.org/doi/10.1021/acs.jnatprod.0c01308>.

¹H and ¹³C NMR spectra of compounds **1–7**; purification of compounds **8–30** from the culture broth and mycelial extracts (PDF)

AUTHOR INFORMATION

Corresponding Author

Vatcharin Rukachaisirikul – Division of Physical Science and Center of Excellence for Innovation in Chemistry, Faculty of Science, Prince of Songkla University, Hat Yai, Songkhla 90112, Thailand; orcid.org/0000-0003-1517-1526; Email: vatcharin.r@psu.ac.th

Authors

Prapatsorn Saetang – Division of Physical Science and Center of Excellence for Innovation in Chemistry, Faculty of Science, Prince of Songkla University, Hat Yai, Songkhla 90112, Thailand

Souwalak Phongpaichit – Division of Biological Science, Faculty of Science, Prince of Songkla University, Hat Yai, Songkhla 90112, Thailand

Sita Preedanon – National Center for Genetic Engineering and Biotechnology (BIOTEC), Klong Luang, Pathumthani 12120, Thailand

Jariya Sakayaroj – School of Science, Walailak University, Thasala, Nakhonsithammarat 80161, Thailand

Sarinya Hadsadee – Department of Chemistry and Center of Excellence for Innovation in Chemistry, Faculty of Science, Ubon Ratchathani University, Ubon Ratchathani 34190, Thailand

Siriporn Jungstittiwong – Department of Chemistry and Center of Excellence for Innovation in Chemistry, Faculty of Science, Ubon Ratchathani University, Ubon Ratchathani 34190, Thailand; orcid.org/0000-0001-5943-6878

Complete contact information is available at:

<https://pubs.acs.org/10.1021/acs.jnatprod.0c01308>

Notes

The authors declare no competing financial interest.

ACKNOWLEDGMENTS

V.R. thanks the NSTDA Chair Professor grant (the fourth Grant) of the Crown Property Bureau and the National Science and Technology Development Agency. P.S. acknowledges the TRF through the Royal Golden Jubilee Ph.D. program (grant number PHD/0211/2559) for a scholarship, the Center of Excellence for Innovation in Chemistry (PERCH-CIC), Ministry of Higher Education, Science, Research and Innovation, the Graduate School and the Division of Physical Science, Faculty of Science, Prince of Songkla University, for partial support. Finally, National Center for Genetic Engineering and Biotechnology (BIOTEC) is acknowledged for the evaluation of cytotoxic activity.

REFERENCES

- (1) Sureram, S.; Wiyakrutta, S.; Ngamrojanavanich, N.; Mahidol, C.; Ruchirawat, S.; Kittakoop, P. *Planta Med.* **2012**, *78*, 582–588.
- (2) Sureram, S.; Kesornpun, C.; Mahidol, C.; Ruchirawat, S.; Kittakoop, P. *RSC Adv.* **2013**, *3*, 1781–1788.
- (3) Klaiklay, S.; Rukachaisirikul, V.; Aungphao, W.; Phongpaichit, S.; Sakayaroj, J. *Tetrahedron Lett.* **2016**, *57*, 4348–4351.
- (4) Phainuphong, P.; Rukachaisirikul, V.; Phongpaichit, S.; Preedanon, S.; Sakayaroj, J. *Tetrahedron* **2017**, *73*, 5920–5925.
- (5) Phainuphong, P.; Rukachaisirikul, V.; Phongpaichit, S.; Sakayaroj, J.; Kanjanasirirat, P.; Borwornpinyo, S.; Akrimajirachote, N.; Yimmual, C.; Muangprasat, C. *Tetrahedron* **2018**, *74*, 5691–5699.
- (6) Kawahara, N.; Nakajima, S.; Satoh, Y.; Yamazaki, M.; Kawai, K.-I. *Chem. Pharm. Bull.* **1988**, *36*, 1970–1975.

(7) Cao, S.; Lee, A. S. Y.; Huang, Y.; Flotow, H.; Ng, S.; Butler, M. S.; Buss, A. D. *J. Nat. Prod.* **2002**, *65*, 1037–1038.

(8) Basset, J.-F.; Leslie, C.; Hamprecht, D.; White, A. J. P.; Barrett, A. G. M. *Tetrahedron Lett.* **2010**, *51*, 783–785.

(9) Hamano, K.; Kinoshita-Okami, M.; Hemmi, A.; Sato, A.; Hisamoto, M.; Matsuda, K.; Yoda, K.; Haruyama, H.; Hosoya, T.; Tanzawa, K. *J. Antibiot.* **1992**, *45*, 1195–1201.

(10) Kawahara, N.; Nozawa, K.; Nakajima, S.; Kawai, K.-I. *J. Chem. Soc., Perkin Trans. 1* **1988**, 2611–2614.

(11) Tayone, W. C.; Honma, M.; Kanamaru, S.; Noguchi, S.; Tanaka, K.; Nehira, T.; Hashimoto, M. *J. Nat. Prod.* **2011**, *74*, 425–429.

(12) Barnett, H. L.; Hunter, B. B. *Illustrated Genera of Imperfect Fungi*; Prentice-Hall, Inc., The American Phytopathological Society, USA, 1998.

(13) Trisuwan, K.; Khamthong, N.; Rukachaisirikul, V.; Phongpaichit, S.; Preedanon, S.; Sakayaroj, J. *J. Nat. Prod.* **2010**, *73*, 1507–1511.

(14) Frisch, M. J.; Trucks, G. W.; Schlegel, H. B.; Scuseria, G. E.; Robb, M. A.; Cheeseman, J. R.; Scalmani, G.; Barone, V.; Mennucci, B.; Petersson, G. A.; Nakatsuji, H.; Caricato, M.; Li, X.; Hratchian, H. P.; Izmaylov, A. F.; Bloino, J.; Zheng, G.; Sonnenberg, J. L.; Hada, M.; Ehara, M.; Toyota, K.; Fukuda, R.; Hasegawa, J.; Ishida, M.; Nakajima, T.; Honda, Y.; Kitao, O.; Nakai, H.; Vreven, T.; Montgomery, J. A., Jr.; Peralta, J. E.; Ogliaro, F.; Bearpark, M.; Heyd, J. J.; Brothers, E.; Kudin, K. N.; Staroverov, V. N.; Kobayashi, R.; Normand, J.; Raghavachari, K.; Rendell, A.; Burant, J. C.; Iyengar, S. S.; Tomasi, J.; Cossi, M.; Rega, N.; Millam, J. M.; Klene, M.; Knox, J. E.; Cross, J. B.; Bakken, V.; Adamo, C.; Jaramillo, J.; Gomperts, R.; Stratmann, R. E.; Yazyev, O.; Austin, A. J.; Cammi, R.; Pomelli, C.; Ochterski, J. W.; Martin, R. L.; Morokuma, K.; Zakrzewski, V. G.; Voth, G. A.; Salvador, P.; Dannenberg, J. J.; Dapprich, S.; Daniels, A. D.; Farkas, Ö.; Foresman, J. B.; Ortiz, J. V.; Cioslowski, J.; Fox, D. J. *Gaussian09*; Gaussian Inc.: Wallingford, 2010.

(15) Phongpaichit, S.; Rungjindamai, N.; Rukachaisirikul, V.; Sakayaroj, J. *FEMS Immunol. Med. Microbiol.* **2006**, *48*, 367–372.

(16) Hunt, L.; Jordan, M.; Jesus, M. D.; Wurm, F. M. *Biotechnol. Bioeng.* **1999**, *65*, 201–205.